



HAL
open science

Human blood plasma in capillary-size flow: Revealing hidden elasticity and scale dependence

U. Windberger, Laurence Noirez

► **To cite this version:**

U. Windberger, Laurence Noirez. Human blood plasma in capillary-size flow: Revealing hidden elasticity and scale dependence. 2020. hal-02513618

HAL Id: hal-02513618

<https://hal.science/hal-02513618>

Preprint submitted on 20 Mar 2020

HAL is a multi-disciplinary open access archive for the deposit and dissemination of scientific research documents, whether they are published or not. The documents may come from teaching and research institutions in France or abroad, or from public or private research centers.

L'archive ouverte pluridisciplinaire **HAL**, est destinée au dépôt et à la diffusion de documents scientifiques de niveau recherche, publiés ou non, émanant des établissements d'enseignement et de recherche français ou étrangers, des laboratoires publics ou privés.

Human Blood Plasma in Capillary-size Flow: Revealing Hidden Elasticity and Scale Dependence

U. Windberger¹, L. Noirez^{2*}

¹Center for Biomedical Research, Medical University Vienna, Waehringerguertel 18-20, 1090 Vienna, Austria

²University Paris-Saclay, Laboratoire Léon Brillouin (CEA-CNRS), 91191 Gif-sur-Yvette, Cédex France

The dynamical mechanical analysis of blood generally uses models inspired by conventional flows, assuming scale-independent homogeneous flows and without considering fluid-surface boundary interactions. The present experimental study highlights the pertinence of a non-conventional approach to identify dynamic properties of human blood plasma. A finite shear elastic response (solid-like property) is identified in nearly static conditions, which also depends on the scale (being reinforced at small scales). Therefore, blood plasma is a scale dependent viscoelastic solid that flows over a weak stress threshold. This finding opens new routes for medical diagnosis and device fabrication.

The transport mechanisms of blood in the vasculature face multiple biological, physical, and biochemical parameters that make their flow laws complex, specific, and fascinating. Ninety years after the first works from Fahraeus and Lindqvist [1] showing the decrease of blood viscosity with decreasing tube diameter, numerous in-silico [2-4], ex-vivo [5-8], and in-vivo studies [9-12] shed light on the behavior of blood cells in flow. Bulk blood viscosity results from such behavior through red blood cell (RBC) alignment in the streamlines and mutual elastic cell-cell coupling [13]. The effect of blood viscosity on vascular resistance includes several mechanisms; on one hand blood itself generates processes in the vessel wall. Its flow velocity and the degree of the cell-free layer along the wall determine the endothelial wall shear stress [14,15] needed to adjust the vessel diameter through mechanotransduction [16,17]. Flowing RBCs rhythmically discharge ATP into blood plasma, being a signal for NO production in endothelial cells [18]. RBCs themselves release their NO into the vessel lumen [19], and communicate the metabolic demand of tissues [20,21]. On the other hand, the vascular geometry influences blood properties by the RBC distribution in the vessel cross-section, by the induction of lift forces, and by the addition of pulsations into blood flow along the elastic fibers in the vessel media [4,13,22]. Therefore, blood and vessels must be recognized as a functional unit to regulate the vascular resistance [23]. Their interaction anticipates a well-designed interface.

Considering the huge information available on the molecular interactions between blood and vessel wall [24], it is surprising that the dynamic of the interface is less explored, even though an immobile plasma portion was postulated already 50 years ago [25]. Blood cells do not shear directly along the endothelial cell surface, as there is a fluid layer of significant length in between, which resists compression and local shear stresses [26]. The fluidic blood-wall interface starts with hydrated proteoglycans, hyaluronan, and glycoproteins on the endothelial surface and extends towards the vessel lumen through adhesion of plasma proteins to form the endothelial surface layer (ESL) [26,27]. This 0.5-3.0 μm layer is fragile and its characterization is difficult being tributary of the technique that is used to analyze it [28,29]. It allows passage of leucocytes through it, but re-arranges quickly to its original thickness,

once, the cell has left the layer. It influences the blood flow profile [30] and the RBC-wall interactions [31], often by minimizing the amount of leucocytes, lipoproteins and fibrinogen [32] at close proximity to the endothelium. By mechanical means, the protective role of the ESL is the result of its thickness and viscoelasticity. Pries and coworkers [33] postulated structures forming the layer. But where would these elastic structures come from and how stable are they?

A classical approach to identify viscoelasticity of liquids is rheology. The current state of the art in conventional rheometry consists in measuring the resistance of the fluid to a shear strain while the sample is placed between two metallic surfaces. One surface is animated of an oscillatory motion while the other one is linked to a sensor to measure the shear stress dynamically transmitted from one substrate to the other one by the sample. It is often forgotten that this technique is entirely dependent on the interaction between the sample and the substrate since a good adhesion of the sample on the substrate is needed to transmit the shear forces. Metallic surfaces are highly unphysiological and might not provide the best anchor for blood. Classical rheometry (gap width of 1 mm) also underestimates the importance of the scale. A testing on macroscopic scales will not capture the quality of interaction between the fluid and its boundaries, especially if the elastic layer is thin. We therefore adapted the dynamic characterization of blood plasma to access its true properties.

The methodology includes an optimized stress transfer through the liquid by enhancing the force of interaction of its first molecular layers to the two surfaces in the rheometer. Excellent wetting is a prerequisite to optimize the no-slippage condition [34]. The degree of wetting can be characterized by the method of the contact angle θ (Fig. 1). Different approaches have shown that the slippage propensity is reduced when the contact angle is reduced [34]. Low strain and the reinforcement of the fluid - substrate cohesion enable to access higher viscoelastic moduli, and at small scale revealed the elastic character of ordinary liquids and fluids [35,36]. The improved wetting method combined to a conventional rheometer showed that ordinary liquids (classified Newtonian by classical rheometry) exhibited a solid-like response below an elastic threshold [37,42]. We felt

therefore confident to find such elasticity in blood plasma after removal of cells that usually provide the elasticity [43].

We optimized the plasma – substrate interaction by means of zero-porosity alumina surfaces. Alumina is chemically and biologically inert and provides a high-energy surface. Blood plasma contains 90% water and must exhibit total wetting (illustrated schematically in Fig. 1) on it. Therefore, the applied experimental conditions are as much as possible non-dissipative for low strain measurements to minimize the no-slippage condition. In rheometry, the shear stress $\sigma(\omega)$ that had to be transmitted through the sample is a synchronic function of the input shear strain wave: $\sigma(\omega) = \gamma_0 \cdot \sin(\omega t + \Delta\phi)$, where γ_0 is a small strain amplitude, ω is the frequency, and $\Delta\phi$ is the phase shift between the input and output signals. The shear stress is transmitted along a path in the fluid thickness. The response measured in a strain range where the response is proportional to the applied strain (linear response) is conventionally expressed in terms of elastic (G') and viscous (G'') moduli that characterize the dynamic properties: $\sigma(\omega) = \gamma_0 \cdot (G'(\omega) \cdot \sin(\omega t) + G''(\omega) \cdot \cos(\omega t))$ (see Fig. 2). We also investigated the effect of fluid thickness, to see if the elastic behavior could be more pronounced when the fluid thickness scales down towards the arteriolar diameter. After giving informed consent (EK Nr. 2114/2019), blood was obtained from a healthy volunteer by puncturing the antecubital vein with a 21G butterfly needle that was connected to a vacutainer system (Greiner Bio-One, Austria), containing EDTA for anticoagulation. Whole blood was centrifuged to obtain platelet-depleted plasma (2310g for 30 minutes) and cooled until assayed. Samples were tested in a ceramic plate-plate (40 mm diameter) environment at ambient temperature using an ARES2 rheometer (TA Instruments, USA).

In our hands blood plasma could be measured at nearly static conditions, and due to the improved cohesion to the plates we were able to identify it as a viscoelastic solid whose elasticity improved at lower sample thickness. The results are shown in detail in the following.

Figure 3 displays the dynamic response of a 0.300mm thickness blood plasma sample submitted to an oscillatory shear sine input over a wide frequency range (0.04 rad/s – 100 rad/s). Low strain amplitude conditions were applied (1.5%) to test the fluid in nearly equilibrium conditions. The elastic modulus G' dominated the dynamic response indicating that plasma responds nearly instantaneously to the oscillatory strain field within this frequency. Viscous dissipation was low, since G'' exhibited values 3 times lower than G' . This means that plasma did not flow but oscillated as a whole at the same frequency at which it was excited. Both moduli increased at higher frequency, indicating a reinforcement of the strength at faster motions.

To test the resistance of the shear elastic response to a mechanical stress, the response of blood plasma was examined as a function of the strain amplitude. The chosen frequency corresponded to the resting heart rate (10 rad/s). Figure 4 displays the evolution of the shear elasticity at room temperature as a function of the strain amplitude at small (0.300 mm) and large (1.100 mm) scales. Three regimes are

distinguished. At low strain amplitude ($\gamma < 200$ %), the shear elastic modulus $G'(\omega)$ was higher than the shear viscous modulus $G''(\omega)$. The viscous component (G'') contributed to about 20 % of the total modulus given by $G = \sqrt{G'^2 + G''^2}$. At higher strain amplitudes ($300 \% < \gamma < 500$ %), both moduli collapsed with a more pronounced fall for $G'(\omega)$, leading to a crossover, which marks the change of behavior from solid-like to viscous-like. At very high strain amplitude ($\gamma > 600$ %), the viscous modulus dominated and the elastic component became negligible (less than 1% of $G''(\omega)$). Viscous behavior was present in the high strain amplitude regime only. Prior to it, blood plasma exhibited an elastic-like regime.

Since the lowest strain amplitudes correspond to less perturbing conditions, the elastic response is the fundamental response of the fluid. In contrast, the viscous flow is the dynamic response produced by the asymptotic vanishing of the shear elasticity at high strain amplitudes. Similar strain dependence schemes have been reported in simple liquids and viscoelastic fluids (polymer melts, glass formers) by different authors [35-42]. The elastic regime is accessible by applying near equilibrium strain conditions, which is possible only under low strain and high wetting substrate. At high strain amplitudes this behavior is quickly lost in favor of apparent flow behavior. The fragility of this solid-like response underlines the experimental difficulty to access to the fundamental elastic response of blood plasma in former studies.

Amplitude sweep tests carried out at different sample thicknesses show that the elastic response was accessible up to 0.300 mm using optimized wetting conditions, but decreased with increasing gap width. At larger sample thicknesses the elastic response vanished. The shear elastic response is therefore lost at high strain amplitudes and large thicknesses. This means that such conditions are away from equilibrium conditions of blood plasma. Figure 5a summarizes the evolution of the shear elasticity of the sample as a function of its thickness. Figure 5b shows the G' -values at near-linear response. As explained above, the elastic plateau developed at very low strains ($\gamma < 5$ %) and decreased until both moduli drop abruptly at about 300 %, at which strain the sample yielded (compare also with Fig. 4). After yielding, the shear elastic moduli converged and became indistinguishable from values measured at other gap thicknesses. The sample exhibited a strong non-linear behavior, and shear elasticity reached asymptotic behavior, typical for a large scale. Blood flow therefore needs large strain amplitudes or large vessel diameters to ensure conditions for an asymptotic behavior and a collapse of shear elasticity in the center of the bloodstream.

In conclusion, we have revealed that platelet depleted plasma exhibits a finite shear elastic response within a frequency range that covers the human heart rate. Its response to an oscillatory shear stress excitation in nearly static conditions (down to 0.04 rad/s upon applying low strain amplitude perturbation) is fundamentally elastic-like. Thus, for blood plasma to flow, the strain impulse has to overpass an elastic threshold. The Newtonian flow behavior is recovered at large strain amplitudes only, indicating that the classification of blood plasma as a Newtonian fluid is a partial description of its mechanical properties. High flow, high shear rates, and pulsations are

needed to overcome the fundamental elastic property of blood plasma.

Additionally we have demonstrated the dimensional properties of shear elasticity by highlighting its reinforcement by the elastic threshold when the probed volume was reduced. Reciprocally, the elastic behavior progressively collapses at large scale and/or at large strain amplitudes, indicating that the viscous behavior observed at larger scales is an asymptotic behavior resulting from the vanishing of the shear elasticity. The present study does not pretend to mimic the endothelium that is the physiological lining for blood, but evidences that a modification of the boundary surface has deep consequences for blood flow. In the present case, our results highlight the importance of optimizing interfacial fluid/substrate interactions. The identification of blood plasma's shear elasticity is in agreement with other works carried out at small scales on liquid water, heptadecane, glycerol, o-terphenyl, or polymer melts. These experiments were carried out using different methods, but by optimizing the conditions of the motion transfer from the stress source to the fluid [35-42]. This appears as the key point in the dynamic characterization of materials. "Static" shear elasticity in the fluidic state reveals collective properties that involve long-range interactions. These elastic forces must originate from intermolecular interactions, possibly from hydrogen bond interconnectivity. In agreement with the pioneering Derjaguin's works [35], the investigations presented confirm that shear elasticity is a generic property of fluids, including also physiological liquids. The shear elasticity found here cannot be compared to 'conventional' solids characterized by much higher moduli. It is also weak in comparison to the high frequency moduli that were measured in liquids at 73 kHz [35], at intermediate frequencies of 10 MHz [36], or at GHz frequencies [44]. The low frequency elasticity is nevertheless of utmost physiological importance since it tells us that blood plasma resists to weak shear flow. This might explain the retardation of the plasma motion relative to that of RBCs in the peripheral circulation [45]. Since the elasticity increases at low thickness, it will be found predominantly at the proximity of the vessel wall. The contribution of plasma proteins to endothelial surface layer is a well-accepted issue [29,33]. But our finding highlights that this layer is not only fluidic (as recognized so far), but contributes elastically as well. Its thickness scales with the cohesion between the components of plasma and the endothelial glycocalyx underneath (note that enzymatic degradation of the glycocalyx can increase blood flow [30] and the local hematocrit [46]), and with the blood flow velocity. A "static" shear elastic layer supports the transmission of transverse shear waves originating from the flowing blood volume to the endothelium, a matter that was found by theoretical modeling for cells embedded in extracellular matrix [28]. The blood plasma property shown here justifies the large integrity of the intraluminal vascular cell-free layer shown in rat mesenteric arteries [47], and underlines its protective role for the endothelium that has been often discussed previously [27,29,48,49].

LN and UW thank P. Baroni for his instrumental assistance and technical innovations. Part of the content of this paper was shown at the 19th ESR meeting in Portoroz, Slovenia.

The authors contributed equally to this work.

*laurence.noirez@cea.fr.

REFERENCES

1. R. Fahraeus, and T. Lindqvist, The viscosity of the blood in narrow capillary tubes, *Am. J. Physiol.* 96, 526-568 (1931).
2. D. A. Fedosov, B. Caswell, and G. E. Karniadakis, A multiscale red blood cell model with accurate mechanics, rheology, and dynamics, *Biophys. J.* 98, 2215-2225 (2010).
3. M. Abkarian, M. Faivre, and A. Viallat, Swinging of red blood cells under shear flow, *Phys. Rev. Lett.* 98, 188302 (2007).
4. A. Kumar, R. G. Henriquez-Rivera, and M. D. Graham, Flow-induced segregation in confined multicomponent suspensions: effects of particle size and rigidity, *J. Fluid Mech.* 738, 423-462 (2014).
5. E. Kaliviotis, J. M. Sherwood, and S. Balabani, Partitioning of red blood cell aggregates in bifurcating microscale flows, *Scientific Reports* 7, 44563 (2017).
6. G. Tomaiuolo, M. Barra, V. Preziosi, A. Cassinese, B. Rotoli, and S. Guido, Microfluidics analysis of red blood cell membrane viscoelasticity, *Lab on a Chip* 11, 449-454 (2011).
7. L. Lanotte, J. Mauer, S. Mendez, D. A. Fedosov, J. M. Fromental, V. Claveria, F. Nicoud, G. Gompper, and M. Abkarian, Red cells' dynamic morphologies govern blood shear thinning under microcirculatory flow conditions, *Proc. Natl. Acad. Sci. USA* 113, E8207 (2016).
8. G. Mchedlishvili, and N. Maeda, Blood flow structure related to red cell flow: a determinant of blood fluidity in narrow microvessels, *Japan J. Physiol.* 51, 19-30 (2001).
9. J. J. Bishop, P. R. Nance, A. S. Popel, M. Intaglietta, and P. C. Johnson, Relationship between erythrocyte aggregate size and flow rate in skeletal muscle venules, *Am. J. Physiol. Heart Circ. Physiol.* 286, H113-H120 (2004).
10. H. H. Lipowsky, and S. Kovalchek, The distribution of blood rheological parameters in the microvasculature of cat mesentery, *Circ. Res.* 43, 738-749 (1978).
11. J. Zhang, P. C. Johnson, and A. S. Popel, Effects of erythrocyte deformability and aggregation on the cell free layer and apparent viscosity of microscopic blood flows, *Microvasc. Res.* 77, 265-272 (2009).
12. S. Kim, R. L. Kong, A. S. Popel, M. Intaglietta, and P. C. Johnson, Temporal and spatial variations of cell-free layer widths in arterioles, *Am. J. Physiol.* 293, H1526-H1535 (2007).
13. M. Abkarian, and A. Viallat, "Deformability of red blood cells". In: Duprat C, Stone HA, editors. *RSC Soft Matter Vol. 4. Fluid-Structure Interaction in Low-Reynolds-Number Flows*. London, UK: The Royal Society of Chemistry (2016). p. 347-462.
14. F. M. A. Box, R. J. van der Geest, M. C. M. Rutten, J. H. and C. Reiber, The influence of flow, vessel diameter, and non-Newtonian blood viscosity on the wall shear stress in a carotid bifurcation model for unsteady flow, *Investigative Radiology* 40, 277-294 (2005).

15. A. M. Malek, S. L. Alper, and S. Izumo. Hemodynamic shear stress and its role in atherosclerosis, *J. Am. Med. Assoc.* 282, 2035-2042 (1999).
16. S. Weinbaum, X. Zhang, Y. Han, H. Vink, and S. C. Cowin, Mechanotransduction and flow across the endothelial glycocalyx, *Proc. Natl. Acad. Sci. USA* 100, 7988–7995 (2003).
17. P. F. Davies, Flow-mediated endothelial mechanotransduction, *Physiol. Rev.* 75, 519-560 (1995).
18. H. Chu, M. M. McKenna, N. A. Krump, S. Zheng, L. Mendelsohn, S. L. Thein, L. J. Garrett, and D. M. Bodine, Low PS. Reversible binding of hemoglobin to band 3 constitutes the molecular switch that mediates O₂ regulation of erythrocyte properties, *Blood* 128, 2708-2716 (2016).
19. S. Nagarajan, R. R. Kadarkarai, V. Saravanakumar, U. M. Balaguru, J. Behera, V. K. Rajendran, Y. Shathya, B. M. J. Ali, V. Sumantran, and S. Chatterjee, Mechanical perturbations trigger endothelial nitric oxide synthase activity in human red blood cells, *Scientific Reports* 6, 26935 (2016).
20. J. C. Arciero, B. E. Carlson, and T. W. Secomb, Theoretical model of metabolic blood flow regulation: roles of ATP release by red blood cells and conducted responses, *Am. J. Physiol. Heart Circ. Physiol.* 295, H156271 (2008).
21. M. I. Ellsworth, The red blood cell as an oxygen sensor: what is the evidence? *Acta Physiol. Scand.* 168, 551-559 (2000).
22. F. N. van de Vosse, and N. Stergiopoulos, Pulse wave propagation in the arterial tree, *Annual Rev. Fluid Mech.* 43, 467-499 (2010).
23. B. E. Carlson, J. C. Arciero, and T. W. Secomb, Theoretical model of blood flow autoregulation: roles of myogenic, shear-dependent, and metabolic responses, *Am. J. Physiol.* 295, H1572-H1579 (2008).
24. C. H. Hesh, Y. Qiu, and W. A. Lam, Vascularized microfluidics and the blood-endothelium interface, *Micromachines* 11, 18-45 (2020).
25. A. L. Copley, Hemorheological aspects of the endothelium-plasma interface, *Microvasc. Res.* 8, 192-212 (1974).
26. H. Vink, and B. R. Duling, Identification of distinct luminal domains for macromolecules, erythrocytes, and leukocytes within mammalian capillaries, *Circ. Res.* 79, 581–589 (1996).
27. S. Weinbaum, J. M. Tarbell, and E. R. Damiano, The structure and function of the endothelial glycocalyx layer, *Annual Rev. Biomed. Eng.* 9, 121–167 (2007).
28. J. M. Tarbell, and Z. D. Shi, Effect of the glycocalyx layer on transmission of interstitial flow shear stress to embedded cells, *Biomech. Model Mechanobiol.* 12, 111–121 (2013).
29. M. Gouverneur, B. van den Berg, M. Nieuwdorp, E. Stroes, and H. Vink, Vasculoprotective properties of the endothelial glycocalyx: effects of fluid shear stress, *J. Internal Medicine* 259, 393-400 (2006).
30. O. Yalcin, V. P. Jani, P. C. Johnson, and P. Cabrales, Implications enzymatic degradation of the endothelial glycocalyx on the microvascular hemodynamics and the arteriolar red cell free layer of the rat cremaster muscle, *Frontiers Physiology* 9, 168 (2018).
31. P. M. McClatchey, M. Schafer, K. S. Hunter, and J. E. Reusch. The endothelial glycocalyx promotes homogenous blood flow distribution within the microvasculature, *Am. J. Phys. Heart Circ. Physiol.* 311, H168–H176 (2016).
32. P. Goerog, and G. V. R. Born, Increased uptake of circulating low-density lipoproteins and fibrinogen by arterial walls after removal of sialic acids from their endothelial surface, *Br. J. Exp. Pathol.* 63, 447–451 (1982).
33. A. R. Pries, T. W. Secomb, and P. Gaehtgens, The endothelial surface layer, *Europ. J. Physiol.* 440, 653-666 (2000).
34. T. D. Blake, Slip between a liquid and a solid: D.M. Tolstoi's (1952) theory reconsidered, *Colloids Surf.* 47, 135-145 (1990).
35. B. V. Derjaguin, U. V. Bazaron, Kh. D. Lamazhapova, and B. D. Tsidypov, Shear elasticity of low-viscosity liquids at low frequencies, *Phys. Rev. A* 42, 2255 (1990).
36. A. Bund, and G. Schwitzgebel, Viscoelastic properties of low-viscosity liquids studied with thickness-shear mode resonators, *Anal. Chem.* 70, 2584-2588 (1998).
37. P. Lv, Z. Yang, Z. Hua, M. Li, M. Lin, and X. Dong, Measurement of viscosity of liquid in micro-crevice, *Flow Measurement and Instrumentation* 46, 72–79 (2015).
38. L. Noirez, H. Mendil-Jakani, and P. Baroni, The missing parameter in rheology: hidden solid-like correlations in viscous liquids, polymer melts and glass formers, *Polym. Int.* 58, 962-968 (2009).
39. H. Mendil, P. Baroni, and L. Noirez, Solid-like rheological response of non-entangled polymers in the molten state, *Eur. Phys. J. E* 19, 77-85 (2006).
40. L. Noirez, and P. Baroni, Revealing the solid-like nature of glycerol at ambient temperature, *J. Mol. Struct.* 972, 16-21 (2010).
41. L. Noirez, and P. Baroni, Identification of a low-frequency elastic behaviour in liquid water, *J. Phys. Condens. Matter* 24, 372101 (2012).
42. L. Noirez, Importance of interfacial interactions to access shear elasticity of liquids and understand flow. *Oil Gas Sci. Technol. Rev. I. F. P. Energ. Nouv.* 72, 10–17 (2017).
43. G.R. Lazaro, A. Hernandez-Machado, I. Pagonabarraga, Rheology of red blood cells under flow in highly confined microchannels, *Soft Matter* 10, 7195 (2014).
44. F. Scarponi, L. Gomez, D. Fioretto D, and L. Palmeri, Brillouin light scattering from transverse and longitudinal acoustic waves in glycerol, *Phys. Rev. B* 70, 054203 (2004).
45. B. R. Duling, I. H. Sarelius, and W. F. Jackson, A comparison of microvascular estimates of capillary blood flow with direct measurements of total striated muscle flow, *Int. J. Microcirc. Clin. Exp.* 1, 409-424 (1982).
46. C. Desjardins, and B. R. Duling, Heparinase treatment suggests a role for the endothelial cell glycocalyx in regulation of capillary hematocrit, *Am. J. Physiol.* 258, H647–654 (1990). □
47. P. M. van Haaren, E. van Bavel, H. Vink, and J. A. Spaan, Localization of the permeability barrier to solutes in isolated arteries by confocal microscopy, *Am. J. Physiol.* 285, H2848–56 (2003). □
48. B. M. van den Berg, J. A. E. Spaan, T. M. Rolf, and H. Vink, Atherogenic region and diet diminish glycocalyx dimension and increase intima media ratios at the murine

carotid artery bifurcation, Am. J. Physiol. 290, H915–20 (2006). □

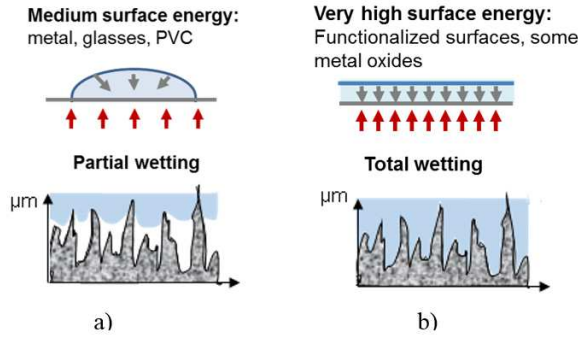


FIG. 1: schemes of partial and total wetting at macroscopic scale (upper figures) and at micron-scale (bottom figures). High-energy surfaces like alumina provide total wetting down to the micron-scale and improve the measurement enabling the access to shear elasticity.

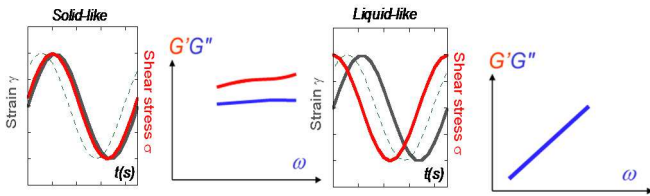


FIG. 2: A general principle to characterize physical properties is to submit the sample to an external stress and to observe its response function. Here, blood plasma is submitted to a mechanical shear strain and we probe its dynamic state via accessing its stress response (in terms of shear elastic (G') and viscous (G'') moduli). When the input signal (here a sinusoidal strain: —) and the output signal (the shear stress: —) are phase-shifted of less than $\Delta\phi < \pi/4$, $G' > G''$ and the material is characterized by a solid-type behavior. A phase shift larger than $\Delta\phi > \pi/4$ indicates that the viscous behavior dominates, $G'' > G'$ (the dashed lines represent $\Delta\phi = \pi/4$ (----)). At $\Delta\phi = \pi/2$, the material exhibits a purely viscous behavior (G'' scales with the frequency and G' becomes negligible).

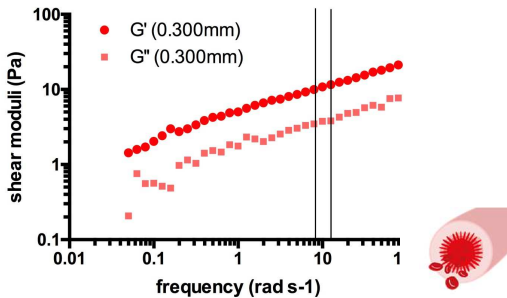


FIG. 3: Dynamic moduli (G' and G'') of a 0.300mm thick blood plasma versus frequency in low strain conditions (total wetting conditions - 1.5 % strain amplitude, room temperature measurements). The vertical lines point out the physiological heartbeat frequency domain (1-1.5 Hz).

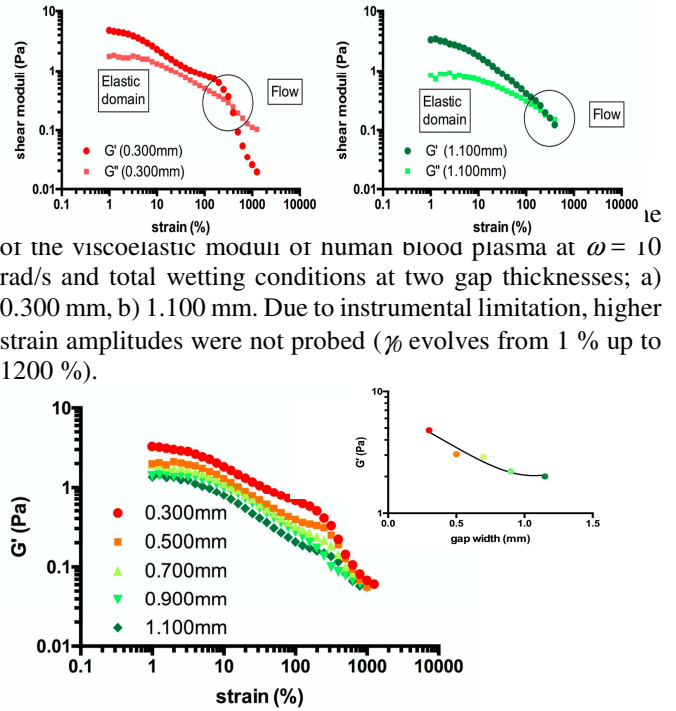


FIG. 4: Evolution of the viscoelastic moduli of human blood plasma at $\omega = 10$ rad/s and total wetting conditions at two gap thicknesses; a) 0.300 mm, b) 1.100 mm. Due to instrumental limitation, higher strain amplitudes were not probed (γ evolves from 1 % up to 1200 %).

FIG. 5: Evolution of the blood plasma shear elasticity measured at different thicknesses from 0.300 mm up to 1.100 mm versus strain amplitude (room temperature measurements, total wetting (alumina surfaces)): ●: 0.300 mm, ■: 0.500 mm, ▲: 0.700 mm, ▼: 0.900 mm, ◆: 1.150 mm. The insert summarizes the evolution of the low strain amplitude shear elasticity (values near to the elastic plateau, logarithmic scale) versus gap thickness.